Published in final edited form as:

IEEE Trans Biomed Eng. 2023 July ; 70(7): 1992–2001. doi:10.1109/TBME.2022.3233345.

Low-Intensity Pulsed Ultrasound Neuromodulation of a Rodent's Spinal Cord Suppresses Motor Evoked Potentials

Yohannes Tsehay[*],
Department of Neurosurgery at the Johns Hopkins University School of Medicine, Baltimore, MD USA.

Yinuo Zeng[*],
Department of Biomedical Engineering at the Johns Hopkins University School of Medicine, Baltimore, MD, USA.

Carly Weber-Levine[*],
Department of Neurosurgery at the Johns Hopkins University School of Medicine, Baltimore, MD USA.

Tolulope Awosika,
Department of Neurosurgery at the Johns Hopkins University School of Medicine, Baltimore, MD USA.

Max Kerensky,
Department of Biomedical Engineering at the Johns Hopkins University School of Medicine, Baltimore, MD, USA.

Andrew M. Hersh,
Department of Neurosurgery at the Johns Hopkins University School of Medicine, Baltimore, MD USA.

Ze Ou,
Department of Biomedical Engineering at the Johns Hopkins University School of Medicine, Baltimore, MD, USA.

Kelly Jiang,
Department of Neurosurgery at the Johns Hopkins University School of Medicine, Baltimore, MD USA.

Meghana Bhimreddy,
Department of Neurosurgery at the Johns Hopkins University School of Medicine, Baltimore, MD USA.

Stuart J. Bauer,
Department of Biomedical Engineering at the Johns Hopkins University School of Medicine, Baltimore, MD, USA.

theodore@jhmi.edu, amir.manbachi@jhu.edu.
Asterisk indicates equal contributions.

The authors declare that there is no conflict of interest.

John N. Theodore*,
Columbia University, New York, NY, USA.

Victor M. Quiroz,
Department of Biomedical Engineering at the Johns Hopkins University School of Medicine, Baltimore, MD, USA.

Ian Suk,
Department of Neurosurgery at the Johns Hopkins University School of Medicine, Baltimore, MD USA.

Safwan Alomari,
Department of Neurosurgery at the Johns Hopkins University School of Medicine, Baltimore, MD USA.

Junfeng Sun,
School of Biomedical Engineering at Shanghai Jiao Tong University, Shanghai, China.

Shanbao Tong,
School of Biomedical Engineering at Shanghai Jiao Tong University, Shanghai, China.

Nitish Thakor,
Department of Biomedical Engineering at the Johns Hopkins University School of Medicine, Baltimore, MD, USA. Department of Biomedical Engineering, National University of Singapore, Singapore; SINAPSE Institute, National University of Singapore, Singapore.

Joshua C. Doloff,
Department of Biomedical Engineering at the Johns Hopkins University School of Medicine, Baltimore, MD; Department of Materials Science and Engineering, Institute for NanoBioTechnology, Johns Hopkins University, Baltimore, MD, USA; Department of Oncology, Division of Cancer Immunology, Sidney Kimmel Comprehensive Cancer Center and the Bloomberg-Kimmel Institute for Cancer Immunotherapy, Translational Tissue Engineering Center, Johns Hopkins University School of Medicine, Baltimore, MD, USA.

Nicholas Theodore,
Department of Neurosurgery at the Johns Hopkins University School of Medicine, Baltimore, MD USA. HEPIUS Innovation Laboratory, affiliated with the Departments of Neurosurgery, Orthopedic Surgery and Biomedical Engineering at the Johns Hopkins University School of Medicine.

Amir Manbachi*
Department of Biomedical Engineering at the Johns Hopkins University School of Medicine, Baltimore, MD, USA.

HEPIUS Innovation Laboratory, affiliated with Departments of Neurosurgery, Biomedical Engineering, Mechanical Engineering, Electrical and Computer Engineering, Anesthesiology and Critical Care Medicine.

Abstract

Objective: Here we investigate the ability of low-intensity ultrasound (LIUS) applied to the spinal cord to modulate the transmission of motor signals.

Methods: Male adult Sprague-Dawley rats (n=10, 250–300 g, 15 weeks old) were used in this study. Anesthesia was initially induced with 2% isoflurane carried by oxygen at 4 L/min via a nose cone. Cranial, upper extremity, and lower extremity electrodes were placed. A thoracic laminectomy was performed to expose the spinal cord at the T11 and T12 vertebral levels. A LIUS transducer was coupled to the exposed spinal cord, and motor evoked potentials (MEPs) were acquired each minute for either 5- or 10-minutes total. Following the sonication period, the ultrasound was turned off and post-sonication MEPs were acquired for an additional 5 minutes.

Results: Hindlimb MEP amplitude significantly decreased during neuromodulation in both the 5- ($p<0.001$) and 10-min ($p=0.004$) sonication cohorts with a corresponding gradual recovery to baseline. Forelimb MEP amplitude did not demonstrate any statistically significant changes during the trial in either the 5-($p=0.46$) or 10-min ($p=0.80$) trials.

Conclusion: LIUS applied to the spinal cord suppresses MEP signals caudal to the site of stimulation, with recovery of MEPs to baseline after sonication.

Significance: LIUS can suppress motor signals in the spinal cord and may be useful in treating movement disorders driven by excessive excitation of spinal neurons.

Keywords

low-intensity pulsed ultrasound; motor evoked potentials; neuromodulation; spinal cord injury; rat model; thoracic spine

I. INTRODUCTION

Ultrasound technology has increasingly been applied to modulate neural activity and can elicit both excitatory and suppressive effects when applied to neural brain tissue [1]. In 1929, E. Newton Harvey observed a modulatory effect of high-frequency sound waves on the beating patterns of turtle and frog hearts [2]. The modulatory effects of ultrasound were later studied using brain tissue, with Fry et al. finding in 1958 that ultrasound focused on the lateral geniculate nucleus of a feline brain could reversibly suppress visual evoked potentials [3]. A ground-breaking work published by Tyler et al. showed that neurons in a brain slice culture can be excited by low-intensity ultrasound (LIUS) [4]. The same group later showed that LIUS has the ability to modulate neural activity in an intact mouse brain [5]. Following their work, many studies showed the ability of LIUS to modulate neural activity in both the central and peripheral nervous systems [6].

In contrast to high-intensity ultrasound, which has been used in tissue ablation, LIUS produces relatively little heat over time with an intensity below 3 W/cm^2 [7]. It has emerged as an effective, safe, and non-invasive tool for the transient modulation of neural activity [8]. Compared with other neuromodulation tools, LIUS can achieve high spatial resolution and deep penetration without requiring any genetic alterations [9]. Preclinical studies in human cortices have found activation and suppression effects without adverse effects [9]–[12]. For example, one recent study demonstrated that repetitive LIUS could induce increased motor cortex excitability lasting up to 30 min, suggesting a good potential of LIUS in clinical interventions for motor disorders [13]. Clinical trials are underway to study LIUS for the

treatment of neurological diseases, including stroke [14], epilepsy [15], [16], Alzheimer's disease [17], and Parkinson's disease [18].

LIUS has predominantly been studied for cranial and peripheral nerve applications, with few studies investigating its effects on spinal cord tissue. One of these studies is from Liao et al., who demonstrated that ultrasound can activate spinal cord neurocircuits and contract the soleus muscle without increasing inflammatory factors [19]. In addition to modulating motor function, LIUS applied to the spinal cord has been reported to reduce neuropathic pain in rats and pigs [20], [21]. LIUS directed at the spinal cord has the potential to help with the treatment of movement disorders, such as dyskinesias. Therefore, we sought to characterize the ability of LIUS applied to the spinal cord to modulate the transmission of motor signals. We hypothesized that LIUS would alter the amplitude of motor evoked potentials (MEPs) in muscle groups distal to the site of stimulation.

II. MATERIALS AND METHODS

A. Animal Preparation

All experimental procedures were approved by the Johns Hopkins University Animal Care and Use Committee and conducted in accordance with the National Institutes of Health guidelines for the care and use of laboratory animals (Protocol #RA20M223). Male adult Sprague-Dawley rats (n=10, 250–300 g, 15 weeks old; Charles River Laboratories) were used in this study and were housed at a temperature of 25°C with a 12/12-h light/dark cycle. Anesthesia was initially induced with 2% isoflurane (Baxter, USA) carried by oxygen at 4 L/min via a nose cone. The rat was placed on a surgical platform with a warming pad placed under the animal and the temperature was maintained at 37 ± 0.5°C throughout the entire experiment.

B. Electrode Placement

The rat was placed on a stereotactic apparatus (Stoelting, USA) and the head was fixed with ear bars. The head of the rat was shaved and a midline incision was made to expose the cranium. Two holes were drilled in the skull over the motor cortex using a standard dental drill (Vogue Professional 6000, USA). Screw electrodes (E363/20, Plastics One, Inc, Roanoke, VA) were inserted 2 mm posterior to the bregma and 2 mm lateral to the midline and were implanted at a depth of 0.75 mm so that they came in contact with the dura without damaging its integrity [22]. Two ground needle electrodes were placed, with one in the soft tissue bulk of the right forelimb and the other in the proximal tail. Two bipolar recording needle electrodes were placed in the soleus of the right hindlimb and in the brachioradialis of the right forelimb (Fig. 1).

C. Surgical Procedures

Following electrode placement, the back of the rat was shaved and a midline incision was made from approximately the T10 to T13 vertebral levels. A muscle dissection was performed to expose the spinous processes, which were then clamped at T10 and T13 by forceps attached to ball joint arms to confer stability. Subperiosteal dissection was

performed to expose the laminae. Laminectomies were performed at T11 and T12 using a high-speed dental drill (Aseptico AEU-10, USA) to expose the spinal cord (Fig. 1).

Following laminectomy, anesthesia was maintained via intraperitoneal injection of ketamine (100 mg/kg) with xylazine (10 mg/kg). All electrodes were then connected to an intraoperative neurophysiological monitoring system (IOM system, Nicolet Biomedical, USA) to record MEPs. The 2 screw electrodes on the skull served as stimulation electrodes, with the left electrode connected to the negative output and the right electrode connected to the positive output. The needle electrode pair at the right hindlimb and right forelimb were used as recording electrodes [22]. The sonication site was at the laminectomy site in the distal thoracic spinal cord.

D. Low-Intensity Ultrasound Neuromodulation

The ultrasound neuromodulation system consists of 2 function generators (Agilent 33250A, Agilent Technologies, USA), an RF amplifier (E&I 240L RF Amplifier, Electronics & Innovation, USA), an ultrasound transducer (Olympus Panametrics V301, USA) and a custom-made cone-shape acoustic collimator. One function generator outputs a square wave to trigger the second function generator, which outputs a sine wave to form a pulsed sine wave signal. The RF amplifier receives the pulsed signal and drives the ultrasound transducer. The acoustic collimator couples the ultrasound beam from the transducer to the target region. The collimator is a custom 3D-printed cone using standard transparent filament with a 1 mm thickness. The diameter of the tip of the cone is 0.5 cm while the diameter that lays flush with the ultrasound transmission is 2.7 cm. The collimator is 5 cm in height. Prior studies have used similar setups [23], [24].

At the time of this study, no prior literature existed on ultrasound interventions for the spinal cord, and parameters were therefore adapted from existing literature of ultrasound neuromodulation in the brain and peripheral nerves [25]–[30]. We chose a fundamental frequency of 500 kHz, which was reported to effectively stimulate the motor cortex [31] and has relatively deep penetration and fine spatial resolution. We chose a tone burst duration of 500 μs and a duty cycle of 50%, which showed bio-effects based on previous studies and our prior experiments [6], [24], [32]. (Fig. 2)

The ultrasound transducer was secured onto the acoustic collimator that was filled with ultrasound gel (Aquasonic 100, Parker Laboratories), and a thin membrane (parafilm, Bemis Company, USA) was attached to the exit plane of the collimator to prevent the gel from leaking or air getting inside. Any visible air bubbles were removed during the assembling process to maximize the coupling. This method was adopted and improved from a prior study [24]. The apparatus was fixed on a probe stand and carefully lowered to the exposed spinal cord (covering T11 and T12). Additional gel interfaced the apex of the collimator and the spinal cord. The probe rested at this fixed location throughout the experiment.

Prior to the experiment, a water tank with a hydrophone (HNR-0500, ONDA corporation, USA) was used to calculate the root-mean-square pressures at the output aperture of the collimator throughout the middle portion of the bursts as 0.0297 MPa, while the instantaneous intensities were 0.060 W/cm^2. This value was optimal as it was similar

to minimum intensities reported in literature to have elicited changes in motor evoked potentials at our chosen fundamental frequency and duty cycle [33]–[37]. This intensity also ensures safety based on prior reported experiments [33], [34]. Finally, we chose 2 sonication durations: 5 and 10 minutes, because we found that it took about 3 to 4 minutes for the MEP amplitude to be maximally suppressed in our preliminary experiments, although the predominant suppression occurs immediately. The 10-min trials were used as a comparison for us to monitor the difference in recovery time following a longer sonication duration.

After setting up the ultrasound neuromodulation system, a 5-min sonication trial was started. All 10 rats received a 5-min sonication trial, and 5 of these rats received an additional 10-min sonication trial. Within each trial were 3 periods: baseline, during-sonication, and post-sonication. In the 5-min sonication trial, the baseline, during-sonication, and post-sonication periods lasted for 1 minute, 5 minutes, and 5 minutes, respectively. In the 10-min sonication trial, the baseline, during-sonication, and post-sonication periods lasted for 2 minutes, 10 minutes, and 5 minutes, respectively (Fig. 3). There was a 30-minute recovery time between the 5- and 10-min trials.

E. Electrophysiology Recording Parameters

The electrical stimulation to induce MEPs was controlled by the IOM system (Nicolet Endeavor CR IOM Machine). To induce one MEP, a train of electrical stimulation consisting of 5 square waves was used. Each square wave lasts 100 μs and waves were separated by 2 ms, resulting in a frequency of 500 Hz. The stimulus intensity was set at 8 mA. This intensity is high enough to induce an obvious MEP without damaging the tissue [22]. Each train of electrical stimulation would induce one MEP signal, and one train was given every second for 20 seconds and then stopped for the following 40 seconds, which ensured that the rat recovered from the electrical stimulation. As a result, each experiment trial was separated into multiple 1-minute windows, and each window was named according to the period and the time point (Fig. 3).

During recording of the MEP signal, a notch filter (60 Hz) was used to eliminate noise. Signals were averaged over 20 signals within each 1-minute window. The signal acquisition was closely monitored to make sure that the MEP amplitude was stable. Baseline MEP was collected only after ensuring the quality and stability of the signal. For the 10-min sonication trial, an additional 1-minute baseline recording was conducted to ensure that the signal was stable after the previous 5-min sonication trial. Following the sonication period, the ultrasound was turned off and post-sonication MEPs were acquired for an additional 5 minutes.

F. Tissue Retrieval for Histology and qPCR

Animals were euthanized at the conclusion of the experiment. Five additional healthy rats had a T11-T12 laminectomy performed and were euthanized to serve as a control group. Their spinal cords were subsequently collected and flash frozen in liquid nitrogen for gene expression analysis or fixed in formalin prior to being processed for paraffin embedding, sectioning, and staining. Frozen samples were transferred to −80°C for storage and later processing.

G. RNA Isolation, Reverse Transcription, and qPCR

Samples from retrieval were removed from the −80°C freezer and placed in liquid nitrogen. To avoid thawing, samples were removed from liquid nitrogen one at a time, transferred to 1 mL TRIzol (Invitrogen) reagent, and homogenized using a PT 2500 E Homogenizer and 12 mm Generator bit (Kinematica). Once all samples were homogenized, RNA isolation was carried out according to the TRIzol Reagent RNA Isolation protocol (Cat#15596018, ThermoFisher). Isolated RNA was resuspended in diethyl pyrocarbonate-treated water. The pellet was solubilized by vortexing and frozen at −80°C.

For reverse transcription, RNA was thawed and quantified by NanoDrop 2000 spectrophotometer (ThermoFisher Scientific). From each sample, 1 μg of RNA was transferred to a polymerase chain reaction (PCR) tube and diluted to a total volume of 12.2 μL with diethyl pyrocarbonate-treated water. High-Capacity cDNA Reverse Transcription kit (ThermoFisher Scientific) and SimpliAmp Thermal Cycler (ThermoFisher Scientific) were used to complete the reverse transcription according to the manufacturer's instructions. Produced cDNA was diluted and stored at −20°C.

For quantitative PCR (qPCR), cDNA, Milli-Q water, 2X Power SYBR Green Master Mix (Applied Biosystems), and 5 μM forward and reverse gene primers were combined and vortexed per vendor instructions. Aliquots of each cDNA-gene solution were transferred to a 384-well qPCR plate for 3 technical replicates per sample. qPCR data was collected via QuantStudio5 (Applied Biosystems).

H. Histology

Retrieved tissue was fixed overnight using 4% paraformaldehyde at 4°C. After fixation, tissues were processed and then paraffin embedded, sectioned at 5 μm thickness and stained according to standard histological (H&E or Masson's Trichrome) methods.

I. Temperature Analysis

To investigate whether the ultrasound sonication induces any thermal effects in the spinal cord, two additional rat spinal cords were collected and fixed in formalin. The spinal cord samples were placed in ultrasound gel and a digital temperature probe (VWR) was inserted into the center of the spinal cord sample. The ultrasound probe was secured directly above the spinal cord and submerged in the ultrasound gel. Temperature was recorded every 10 seconds for 30 minutes. After the first 10 minutes, ultrasound sonication was initiated with the same parameters as described above. The spinal cord samples were sonicated for 10 minutes, before discontinuing and monitoring temperature without sonication for an additional 10 minutes.

J. Data Processing and Statistical Analysis

MEPs were extracted from raw recordings and self-developed MATLAB scripts (MATLAB version 2021b, The Mathworks, Inc.) were used to process the data. The MEP signals were also inspected manually to ensure they contained no obvious artifacts or noises. MEP peak amplitudes and latencies of the positive and negative peaks were measured by searching for the global extremum in the extracted data. Peak amplitude is defined as the difference

between the amplitude of the peak and the average amplitude from the baseline period. Peak latency is defined as the time difference between stimulation onset and the peak. The peak-to-peak amplitude was then calculated by subtracting the negative peak amplitude from the positive peak amplitude. Within each trial, all calculated MEP amplitudes and latencies in each 1-minute window were normalized relative to the baseline of each animal.

The averages of the normalized amplitudes or latencies in all 1-minute windows within each period were calculated for statistical analysis. One-way Kruskal-Wallis tests were performed on the amplitudes and latencies of the 3 periods (BL, DS, PS) in both the 5-min and 10-min trials to test the alternative hypothesis that the measures of the 3 periods were significant, post hoc tests were performed to identify statistically significant differences of the measurements between each pair of periods. Wilcoxon rank sum tests were also performed to compare each of the baseline, during-sonication and post-sonication periods in the 5-min trials to the periods in the 10-min trials. Lastly, a linear regression was fitted to the post-sonication period for both the 5-min and 10-min trials for each animal, and a Wilcoxon rank sum test was performed on the distribution of the recovery slopes in the 2 trials. For qPCR statistical analysis, a two-tailed unpaired T-test with Welch's correction was performed comparing non-stimulated to stimulated tissue. A p-value less than 0.05 was considered statistically significant. Data from the temperature experiment was analyzed in Microsoft Excel.

III. RESULTS

A. Effects of Ultrasound Neuromodulation on Electrophysiology

MEPs were recorded from both the forelimb and the hindlimb in the 5-min (Fig. 4A) and 10-min (Fig. 5A) sonication trials and were depicted as boxplots. There was a large interanimal variance in amplitude, with forelimb and hindlimb having an average and standard deviation of 126.83 mV ± 94.59 mV and 54.95 mV ± 36.39 mV, respectively. Therefore, it was necessary to normalize the amplitude to the animals' baseline values for subsequent analysis. Latency, on the other hand, had minimal interanimal variation with forelimb and hindlimb having an average and standard deviation of 31.71 ms ± 1.68 ms and 35.49 ms ± 2.27 ms, respectively, indicating a proper MEP protocol. In animals that had multiple baseline measurements, there was minimal variation between the two baseline amplitudes with an average coefficient of variance for the forelimb and hindlimb of 14% and 6.8%, respectively. The MEP waveforms were similar to ones reported in prior literature [38], [39] (Fig. 6). An obvious depression of the MEP amplitude in the hindlimb was observed immediately after starting sonication and continued for the duration of the sonication (Fig. 6). The suppressed MEP amplitude recovered gradually during the post-sonication period (Figs. 4E, 5E, and 6). As a comparison, no obvious variation was found in the forelimb MEP amplitude (Figs. 4D, 5D, and 6). In both the 5-min and 10-min trials, forelimb MEP amplitude did not show any statistically significant differences between the three periods ($\chi^2(2)=1.54$, $p=0.46$ for 5-min trials; $\chi^2(2)=0.44$, $p=0.80$ for 10-min trials) (Figs. 4B and 5B). In contrast, hindlimb MEP amplitude showed a statistically significant decrease during neuromodulation, and a gradual recovery to baseline in both 5-min and 10-min sonication trials ($\chi^2(2)=19.17$, $p<0.001$ for 5-min trials; $\chi^2(2)=10.89$, $p<0.01$ for 10-

min trials) (Figs. 4E and 5E). Post hoc analyses showed statistically significant differences between baseline and during-sonication period for the 5- ($p<0.001$) and 10-min ($p<0.01$) trials, and between during-sonication and post-sonication periods for the 5-min cohort ($p<0.01$) while no significant difference resulted in the 10-min case ($p=0.08$) (Figs. 4B and 5B). The difference between baseline and post-sonication was not significant for either the 5- or 10-min trials ($p = 0.46$ for 5-min, $p = 0.53$ for 10-min). Wilcoxon rank sum tests also showed statistically significant differences between forelimb and hindlimb MEP amplitudes in the during-sonication period for both the during-sonication period for both the 5- ($p<0.001$) and 10-min cohorts ($p<0.01$) (Figs. 4B and 5B).

There were 2 outliers in the 5-min forelimb MEP recordings that were 4 standard deviations away from the mean, so the statistical tests were repeated without the outliers as a measure of robustness. These tests illustrated that the sonication effect on forelimb MEPs was not statistically significant even without the outliers ($\chi^2(2)=0.77$, $p=0.68$).

MEP amplitude showed a general recovery after sonication (Fig. 6). The recovery trajectory of each subject was fitted with a linear regression with respect to time, and a Wilcoxon rank-sum test was performed on the distribution of the recovery slope. The test confirmed that there was no statistically significant difference in the recovery speed between the 5- and 10-min trials ($p=0.59$). In the 5-min groups, the fitted line recovered back to baseline after 5 minutes of recovery. However, in the 10-min groups, the fitted line only recovered to 80% of baseline after 5 minutes of recovery. The average recovery speed was 20% of baseline per minute for the 5-min group, and 14% of baseline per minute for the 10-min group.

As for the latencies of both the positive and negative peaks, the only statistically significant difference was between the stages for the 5-min forelimb positive peak and 5-min hindlimb negative peak (5-min forelimb positive peak $\chi^2(2)=7.26$, $p=0.027$, 5-min hindlimb negative peak $\chi^2(2)=6.31$, $p=0.042$) (Figs. 4C and 5C).

B. Safety of Ultrasound Neuromodulation

The safety of LIUS was evaluated via staining of the spinal cord tissue to evaluate for any structural changes as well as qPCR to monitor for any gene expression or phenotype changes. Both the hematoxylin and eosin (H&E) and Masson's Trichome stains showed no detectable structural or morphological changes between the sonicated (n=5) and control groups (n=5) (Fig. 7A). Similarly, the qPCR data also showed no difference between the control and sonicated groups in the immune/inflammatory, neuromodulatory, and fibrosis genes investigated (Fig. 7B). The largest change in gene expression was in the neuromodulatory-associated gene, neurofilament light chain (Nefl), though the difference was not statistically significant ($p=0.0636$).

Thermal effect of the ultrasound sonication was investigated by measuring the change in temperature during ten minutes of sonication of two *ex vivo* spinal cord samples (Fig. 8A). As anticipated, we saw minimal change in the temperature of the spinal cord samples during ten minutes of sonication. For sample 1, the pre-, during-, and post-sonication average temperatures were 18.1°C ± 0.2°C, 18.5°C ± 0.2°C, and 18.4°C ± 0.2°C, respectively. For sample 2, the pre-, during-, and post-sonication temperatures were 17.6°C ± 0.2°C, 18.3°C

± 0.3°C, and 18.6°C ± 0.1°C, respectively. Additionally, the minimal change in temperature occurred very gradually, while the loss of MEPs occurs immediately with sonication (Fig. 7B). Therefore, it is unlikely that thermal effects contributed to the decrease in MEPs seen during sonication.

IV. DISCUSSION

A. Effect of LIUS

The main hypothesis we tested in this paper was that ultrasound neuromodulation on the spinal cord (T11) would alter the hindlimb MEPs while keeping the forelimb MEPs unchanged. Figures 4E and 5E show a significant depression effect of the LIUS on the hindlimb MEP amplitudes, and the statistical analysis also showed significant changes in the hindlimb MEP amplitudes (Fig. 4B and Fig. 5B). The MEP amplitudes were depressed during sonication for both 5-min and 10-min trials. On the other hand, the forelimb MEP amplitudes showed no significant change during sonication. Other than the amplitudes, the MEP latencies of both 5-min and 10-min sonication didn't show significant change. This result indicates that LIUS on the dorsal spinal cord has a depression effect. The unchanged latency indicates that LIUS at our parameters does not affect the nerve conduction velocity. Changes in latency are typically associated with damage to motor pathways, such as demyelination or axonal damage [40]. Therefore, the lack of change in latency highlights the safety of our sonication parameters. The safety was further supported by our histology analysis, which showed no gross damage to the spinal cord or changes in gene expression (Fig. 7). Similarly, our sonication parameters induced minimal change in tissue temperature (Fig. 8).

LIUS applied to the motor cortex has been reported to modulate motor excitability and suppression, with the directionality of the response dependent on the sonication parameters. Yoon et al. reported that high duty cycles and short sonication durations resulted in excitatory effects on the ovine motor cortex [41]. Fomenko et al. inhibited cortical excitability in humans using lower duty cycles and longer sonication duration [14]. The few previous studies on LIUS at the spinal cord level suggest a role in motor excitability. For instance, Liao et al. noted that using an intensity >0.5 MPa can lead to activation of neuronal circuits and soleus muscle recruitment [19]. In contrast, our study is the first to find that LIUS in the spinal cord can induce motor suppression caudal to the site of stimulation.

The inhibitory effect of LIUS may find clinical utility in the treatment of diseases driven by excessive excitation of spinal neurons. For example, spinal segmental myoclonus is a movement disorder manifesting as the rhythmic or semi-rhythmic jerking of limbs and is thought to be caused by dysfunction of inhibitory interneurons within the spinal cord resulting in overactivation of lower motor neurons in the ventral horn [42]. Similarly, stiff-man syndrome likely involves impaired spinal inhibitory glycinergic circuits or GABAergic interneurons, leading to abnormal rigidity and spasms [43]. The inhibitory effect of LIUS may help reduce the neuronal overactivity driving the disease, although more work is needed to understand this clinical potential [44], [45].

B. Mechanisms and Pathways

Despite research efforts, the mechanism behind ultrasound-mediated neuromodulation is not yet clear. At low intensities, thermal effects can lead to perturbation of neuronal activity levels through synaptic changes, decreases in synaptic vesicle count, or expansion of pre- and post-synaptic junctions. Because low intensities do not exhibit significant thermal effects [46], [47], LIUS-mediated neuromodulation is likely explained by non-thermal effects, including acoustic cavitation effects, ion channel permeability alteration, and indirect neuromodulation through membrane deformation [48]. Recent studies have suggested that LIUS exerts acoustic radiation forces that impinge on local ion channels [49]. Ultrasonic waves exert a mechanical energy that can stretch and distort the cell membrane, ultimately affecting the flux of ions through the lipid bilayer. Several different channels including voltage-gated calcium, sodium, and potassium, as well as neurotransmitter receptors, have shown mechanosensitive properties [14], [50]. Other hypotheses of the mechanism behind LIUS remain to be explored.

More work is needed to understand the neuronal tracts or populations affected during LIUS stimulation. The dorsal funiculus of the rat spinal cord contains the fasciculi cuneatis and gracilis superficially and the dorsal corticospinal tract more deeply. The rat corticospinal tract also has a dorsolateral division which projects caudally in the lateral funiculus of the spinal cord. Morris et al. suggested that the dorsolateral division of the corticospinal tract contributes major input to ventral horn cells [51]. However, it is unknown which of these tracts is responsible for the effect observed in this study, and the unique functions of the divisions of the rat corticospinal tract are a current topic of investigation. Knowledge of the neuronal population responsible for loss of MEPs observed in this study can facilitate the ability to precisely stimulate a cross-sectional segment of the spinal cord, allowing specific targeting of spinal cord tissue responsible for the clinical manifestations of movement disorders. High spatial resolution and precision in the targeting of LIUS neuromodulation is important for clinical translation, as the spinal cord is a functionally dense organ. Insufficient spatial resolution could result in modulation of neurons that are not involved in disease pathophysiology.

C. Limitations

Our transducer technology requires that the animal be fully anesthetized for neuromodulation. Notably, the degree of anesthesia may influence the neuromodulatory effects of LIUS and the ability to transmit motor commands [52]. Although the upper limb MEPs provided a control, future studies should standardize the observed effect through a constant influx of anesthesia, potentially through a ketamine/xylazine drip into the femoral vein. Additionally, although MEPs serve as useful proxies for motor commands, studies examining motor function in a conscious animal are needed. A compact and portable transducer and amplifier can be developed to be implanted over the spinal cord and stimulate the cord during active movement [14]. Importantly, our electrophysiology machine, the Nicolet Endeavor CR IOM Machine, is a clinical machine that only allowed for the export of the averaged potential traces at each time point. In future studies, it may be helpful to analyze the individual traces prior to looking at the averaged traces. Additionally, animals were euthanized upon the conclusion of the experiment and were not monitored over

time. We did not find evidence of nerve damage as assessed by neuromotor function, electrophysiology, H&E staining, Nissl staining, and protein expression following LIUS treatment, but longer survival times are needed to determine the long-term safety of LIUS spinal cord stimulation. Finally, our experimental setup requires a laminectomy as the posterior bony elements of the spinal column can interfere with the neuromodulatory capabilities of ultrasound waves. However, LIUS has been performed transcranially [50], and external LIUS has been performed on rodents and pigs [19], [53], demonstrating successful noninvasive modulation of sensory and motor circuits in the spine. In future studies, we hope to adapt our LIUS transducer technology to achieve the same suppression of MEPs without requiring exposure of the spinal cord.

V. CONCLUSION

LIUS neuromodulation at a center frequency of 500 kHz, tone burst duration of 500 μs, and duty cycle of 50% with sonication times of 5- or 10-minutes causes transient suppression of MEP signals. Histology and qPCR demonstrate that the neuromodulation does not cause damage to the tissue while temperature analysis indicates minimal change in tissue temperature during sonication.

ACKNOWLEDGMENT

This work was supported by funding from Defense Advanced Research Projects Agency, DARPA, Award Contract #: N660012024075. In addition, AM acknowledges funding support from Johns Hopkins Institute for Clinical and Translational Research's Clinical Research Scholars Program (KL2), administered by the National Center for Advancing Translational Sciences, National Institute of Health. We thank the Johns Hopkins Research Animal Resources and the Defense Advanced Research Projects Agency (DARPA) for their continued support our work.

Yohannes Tsehay acknowledges funding from NREF for this work. Nicholas Theodore and Amir Manbachi acknowledge funding support from Defense Advanced Research Projects Agency, DARPA, Award Contract #: N660012024075.

REFERENCES

[1]. Jiang X et al. , "A Review of Low-Intensity Pulsed Ultrasound for Therapeutic Applications," IEEE Trans Biomed Eng, vol. 66, no. 10, pp. 2704–2718, Oct. 2019, doi: 10.1109/TBME.2018.2889669. [PubMed: 30596564]

[2]. Harvey EN, "THE EFFECT OF HIGH FREQUENCY SOUND WAVES ON HEART MUSCLE AND OTHER IRRITABLE TISSUES," 10.1152/ajplegacy.1929.91.1.284, vol. 91, no. 1, pp. 284–290, Dec. 1929, doi: 10.1152/AJPLEGACY.1929.91.1.284.

[3]. Fry FJ, Ades HW, and Fry WJ, "Production of Reversible Changes in the Central Nervous System by Ultrasound," Science (1979), vol. 127, no. 3289, pp. 83–84, Jan. 1958, doi: 10.1126/SCIENCE.127.3289.83.

[4]. Tyler WJ, Tufail Y, Finsterwald M, Tauchmann ML, Olson EJ, and Majestic C, "Remote Excitation of Neuronal Circuits Using Low-Intensity, Low-Frequency Ultrasound," PLoS One, vol. 3, no. 10, p. e3511, Oct. 2008, doi: 10.1371/JOURNAL.PONE.0003511. [PubMed: 18958151]

[5]. Tufail Y et al. , "Transcranial Pulsed Ultrasound Stimulates Intact Brain Circuits," Neuron, vol. 66, no. 5, pp. 681–694, Jun. 2010, doi: 10.1016/J.NEURON.2010.05.008. [PubMed: 20547127]

[6]. Baek H, Pahk KJ, and Kim H, "A review of low-intensity focused ultrasound for neuromodulation," Biomed Eng Lett, vol. 7, no. 2, p. 135, May 2017, doi: 10.1007/S13534-016-0007-Y. [PubMed: 30603160]

[7]. Xin Z, Lin G, Lei H, Lue TF, and Guo Y, “Clinical applications of low-intensity pulsed ultrasound and its potential role in urology,” Transl Androl Urol, vol. 5, no. 2, p. 255, Apr. 2016, doi: 10.21037/TAU.2016.02.04. [PubMed: 27141455]

[8]. Wang P, Zhang J, Yu J, Smith C, and Feng W, “Brain Modulatory Effects by Low-Intensity Transcranial Ultrasound Stimulation (TUS): A Systematic Review on Both Animal and Human Studies,” Front Neurosci, vol. 13, no. JUL, 2019, doi: 10.3389/FNINS.2019.00696.

[9]. Liu X, Qiu F, Hou L, and Wang X, “Review of Noninvasive or Minimally Invasive Deep Brain Stimulation,” Front Behav Neurosci, vol. 15, p. 373, Jan. 2022, doi: 10.3389/FNBEH.2021.820017/BIBTEX.

[10]. Fomenko A et al. , “Systematic examination of low-intensity ultrasound parameters on human motor cortex excitability and behaviour,” Elife, vol. 9, pp. 1–68, Oct. 2020, doi: 10.7554/ELIFE.54497.

[11]. Lee W et al. , “Transcranial focused ultrasound stimulation of human primary visual cortex,” Scientific Reports 2016 6:1, vol. 6, no. 1, pp. 1–12, Sep. 2016, doi: 10.1038/srep34026.

[12]. Legon W et al. , “Transcranial focused ultrasound modulates the activity of primary somatosensory cortex in humans,” Nature Neuroscience 2013 17:2, vol. 17, no. 2, pp. 322–329, Jan. 2014, doi: 10.1038/nn.3620.

[13]. Zhang Y, Ren L, Liu K, Tong S, Yuan TF, and Sun J, “Transcranial ultrasound stimulation of the human motor cortex,” iScience, vol. 24, no. 12, Dec. 2021, doi: 10.1016/J.ISCI.2021.103429.

[14]. Fomenko A, Neudorfer C, Dallapiazza RF, Kalia SK, and Lozano AM, “Low-intensity ultrasound neuromodulation: An overview of mechanisms and emerging human applications,” Brain Stimul, vol. 11, no. 6, pp. 1209–1217, Nov. 2018, doi: 10.1016/J.BRS.2018.08.013. [PubMed: 30166265]

[15]. Zhang M et al. , “Low-Intensity Focused Ultrasound-Mediated Attenuation of Acute Seizure Activity Based on EEG Brain Functional Connectivity,” Brain Sci, vol. 11, no. 6, Jun. 2021, doi: 10.3390/BRAINSCI11060711.

[16]. Bubrick EJ, Mcdannold NJ, White PJ, and Bubrick E, “Low Intensity Focused Ultrasound for Epilepsy- A New Approach to Neuromodulation:,” 10.1177/15357597221086111, vol. 2022, no. 0, p. 153575972210861, Mar. 2022, doi: 10.1177/15357597221086111.

[17]. Meng Y, Volpini M, Black S, Lozano AM, Hynynen K, and Lipsman N, “Focused ultrasound as a novel strategy for Alzheimer disease therapeutics,” Ann Neurol, vol. 81, no. 5, pp. 611–617, May 2017, doi: 10.1002/ANA.24933. [PubMed: 28395123]

[18]. Lee KS, Clennell B, Steward TGJ, Gialeli A, Cordero-Llana O, and Whitcomb DJ, “Focused Ultrasound Stimulation as a Neuromodulatory Tool for Parkinson’s Disease: A Scoping Review,” Brain Sci, vol. 12, no. 2, p. 289, Feb. 2022, doi: 10.3390/BRAINSCI12020289/S1. [PubMed: 35204052]

[19]. Liao YH et al. , “Effects of Noninvasive Low-Intensity Focus Ultrasound Neuromodulation on Spinal Cord Neurocircuits in Vivo,” Evidence-based Complementary and Alternative Medicine, vol. 2021, 2021, doi: 10.1155/2021/8534466.

[20]. Uddin SMZ, Komatsu DE, Motyka T, and Petterson S, “Low-Intensity Continuous Ultrasound Therapies—A Systematic Review of Current State-of-the-Art and Future Perspectives,” Journal of Clinical Medicine 2021, Vol. 10, Page 2698, vol. 10, no. 12, p. 2698, Jun. 2021, doi: 10.3390/JCM10122698.

[21]. Arulpragasam AR, van ‘t Wout-Frank M, Barredo J, Faucher CR, Greenberg BD, and Philip NS, “Low Intensity Focused Ultrasound for Non-invasive and Reversible Deep Brain Neuromodulation—A Paradigm Shift in Psychiatric Research,” Front Psychiatry, vol. 13, p. 112, Feb. 2022, doi: 10.3389/FPSYT.2022.825802/BIBTEX.

[22]. Iyer S, Maybhate A, Presacco A, and All AH, “Multi-limb acquisition of motor evoked potentials and its application in spinal cord injury,” J Neurosci Methods, vol. 193, no. 2, pp. 210–216, Nov. 2010, doi: 10.1016/J.JNEUMETH.2010.08.017. [PubMed: 20832429]

[23]. Tufail Y, Yoshihiro A, Pati S, Li MM, and Tyler WJ, “Ultrasonic neuromodulation by brain stimulation with transcranial ultrasound,” Nature Protocols 2011 6:9, vol. 6, no. 9, pp. 1453–1470, Sep. 2011, doi: 10.1038/nprot.2011.371.

[24]. Zeng Y et al., “A MINIATURE LASER SPECKLE CONTRAST IMAGER FOR MONITORING OF THE NEURO-MODULATORY EFFECT OF TRANSCRANIAL FOCUSED ULTRASOUND STIMULATION”, doi: 10.1115/dmd2021-1038.

[25]. Min B-K et al. , “Focused ultrasound-mediated suppression of chemically-induced acute epileptic EEG activity,” BMC Neuroscience 2011 12:1, vol. 12, no. 1, pp. 1–12, Mar. 2011, doi: 10.1186/1471-2202-12-23.

[26]. King RL, Brown JR, Newsome WT, and Pauly KB, “Effective Parameters for Ultrasound-Induced In Vivo Neurostimulation,” Ultrasound Med Biol, vol. 39, no. 2, pp. 312–331, Feb. 2013, doi: 10.1016/J.ULTRASMEDBIO.2012.09.009. [PubMed: 23219040]

[27]. Yoo SS et al. , “Focused ultrasound modulates region-specific brain activity,” Neuroimage, vol. 56, no. 3, pp. 1267–1275, Jun. 2011, doi: 10.1016/J.NEUROIMAGE.2011.02.058. [PubMed: 21354315]

[28]. Plaksin M, Kimmel E, and Shoham S, “Cell-Type-Selective Effects of Intramembrane Cavitation as a Unifying Theoretical Framework for Ultrasonic Neuromodulation,” eNeuro, vol. 3, no. 3, pp. 229–244, May 2016, doi: 10.1523/ENEURO.0136-15.2016.

[29]. Guo T et al. , “Pulsed transcranial ultrasound stimulation immediately after the ischemic brain injury is neuroprotective,” IEEE Trans Biomed Eng, vol. 62, no. 10, pp. 2352–2357, Oct. 2015, doi: 10.1109/TBME.2015.2427339. [PubMed: 25935023]

[30]. Li H, Sun J, Zhang D, Omire-Mayor D, Lewin PA, and Tong S, “Low-intensity (400 mW/cm2, 500 kHz) pulsed transcranial ultrasound preconditioning may mitigate focal cerebral ischemia in rats,” Brain Stimul, vol. 10, no. 3, pp. 695–702, May 2017, doi: 10.1016/J.BRS.2017.02.008. [PubMed: 28279642]

[31]. King RL, Brown JR, Newsome WT, and Pauly KB, “Effective parameters for ultrasound-induced in vivo neurostimulation,” Ultrasound Med Biol, vol. 39, no. 2, pp. 312–331, 2013, doi: 10.1016/J.ULTRASMEDBIO.2012.09.009. [PubMed: 23219040]

[32]. Wang P, Zhang J, Yu J, Smith C, and Feng W, “Brain Modulatory Effects by Low-Intensity Transcranial Ultrasound Stimulation (TUS): A Systematic Review on Both Animal and Human Studies,” Brain Modulatory Effects by Low-Intensity Transcranial Ultrasound Stimulation (TUS): A Systematic Review on Both Animal and Human Studies. Front. Neurosci, vol. 13, p. 696, 2019, doi: 10.3389/fnins.2019.00696.

[33]. Tufail Y et al. , “Transcranial Pulsed Ultrasound Stimulates Intact Brain Circuits,” Neuron, vol. 66, no. 5, pp. 681–694, Jun. 2010, doi: 10.1016/J.NEURON.2010.05.008. [PubMed: 20547127]

[34]. Liao YH et al. , “Effects of Noninvasive Low-Intensity Focus Ultrasound Neuromodulation on Spinal Cord Neurocircuits in Vivo,” Evidence-based Complementary and Alternative Medicine, vol. 2021, 2021, doi: 10.1155/2021/8534466.

[35]. Sato T, Shapiro MG, and Tsao DY, “Ultrasonic Neuromodulation Causes Widespread Cortical Activation via an Indirect Auditory Mechanism,” Neuron, vol. 98, no. 5, pp. 1031–1041.e5, Jun. 2018, doi: 10.1016/J.NEURON.2018.05.009. [PubMed: 29804920]

[36]. Guo T et al. , “Pulsed transcranial ultrasound stimulation immediately after the ischemic brain injury is neuroprotective,” IEEE Trans Biomed Eng, vol. 62, no. 10, pp. 2352–2357, Oct. 2015, doi: 10.1109/TBME.2015.2427339. [PubMed: 25935023]

[37]. Tyler WJ, Tufail Y, Finsterwald M, Tauchmann ML, Olson EJ, and Majestic C, “Remote Excitation of Neuronal Circuits Using Low-Intensity, Low-Frequency Ultrasound,” PLoS One, vol. 3, no. 10, p. e3511, Oct. 2008, doi: 10.1371/JOURNAL.PONE.0003511. [PubMed: 18958151]

[38]. Iyer S, Maybhate A, Presacco A, and All AH, “Multi-limb acquisition of motor evoked potentials and its application in spinal cord injury,” J Neurosci Methods, vol. 193, no. 2, pp. 210–216, Nov. 2010, doi: 10.1016/J.JNEUMETH.2010.08.017. [PubMed: 20832429]

[39]. Nashmi R, Imamura H, Tator CH, and Fehlings MG, “Serial Recording of Somatosensory and Myoelectric Motor Evoked Potentials: Role in Assessing Functional Recovery after Graded Spinal Cord Injury in the Rat,” https://home.liebertpub.com/neu, vol. 14, no. 3, pp. 151–159, Jan. 2009, doi: 10.1089/NEU.1997.14.151.

[40]. Kallioniemi E, Pitkänen M, Säisänen L, and Julkunen P, "Onset Latency of Motor Evoked Potentials in Motor Cortical Mapping with Neuronavigated Transcranial Magnetic Stimulation," Open Neurol J, vol. 9, pp. 62–69, 2015. [PubMed: 26535068]

[41]. Yoon K et al. , "Effects of sonication parameters on transcranial focused ultrasound brain stimulation in an ovine model," PLoS One, vol. 14, no. 10, p. e0224311, Oct. 2019, doi: 10.1371/JOURNAL.PONE.0224311.

[42]. Termsarasab P, Thammongkolchai T, and Frucht SJ, "Spinal-generated movement disorders: a clinical review," J Clin Mov Disord, vol. 2, no. 1, Dec. 2015, doi: 10.1186/S40734-015-0028-1.

[43]. Floeter MK, Valls-Solé J, Toro C, Jacobowitz D, and Hallett M, "Physiologic studies of spinal inhibitory circuits in patients with stiff-person syndrome," Neurology, vol. 51, no. 1, pp. 85–93, 1998, doi: 10.1212/WNL.51.1.85. [PubMed: 9674784]

[44]. Wainger BJ et al. , "Effect of Ezogabine on Cortical and Spinal Motor Neuron Excitability in Amyotrophic Lateral Sclerosis: A Randomized Clinical Trial," JAMA Neurol, vol. 78, no. 2, pp. 186–196, Feb. 2021, doi: 10.1001/JAMANEUROL.2020.4300. [PubMed: 33226425]

[45]. Collins MN, Legon W, and Mesce KA, "The Inhibitory Thermal Effects of Focused Ultrasound on an Identified, Single Motoneuron," eNeuro, vol. 8, no. 2, Mar. 2021, doi: 10.1523/ENEURO.0514-20.2021.

[46]. ter Haar G, "Therapeutic applications of ultrasound," Prog Biophys Mol Biol, vol. 93, no. 1–3, pp. 111–129, Jan. 2007, doi: 10.1016/J.PBIOMOLBIO.2006.07.005. [PubMed: 16930682]

[47]. O'Brien WD, "Ultrasound–biophysics mechanisms," Prog Biophys Mol Biol, vol. 93, no. 1–3, pp. 212–255, Jan. 2007, doi: 10.1016/J.PBIOMOLBIO.2006.07.010. [PubMed: 16934858]

[48]. Tyler WJ, Lani SW, and Hwang GM, "Ultrasonic modulation of neural circuit activity," Curr Opin Neurobiol, vol. 50, pp. 222–231, Jun. 2018, doi: 10.1016/J.CONB.2018.04.011. [PubMed: 29674264]

[49]. Kubanek J, Shi J, Marsh J, Chen D, Deng C, and Cui J, "Ultrasound modulates ion channel currents," Sci Rep, vol. 6, Apr. 2016, doi: 10.1038/SREP24170.

[50]. Baek H, Pahk KJ, and Kim H, "A review of low-intensity focused ultrasound for neuromodulation," Biomed Eng Lett, vol. 7, no. 2, pp. 135–142, May 2017, doi: 10.1007/S13534-016-0007-Y. [PubMed: 30603160]

[51]. Morris R and Whishaw IQ, "A proposal for a rat model of spinal cord injury featuring the rubrospinal tract and its contributions to locomotion and skilled hand movement," Front Neurosci, vol. 10, no. JAN, p. 5, 2016, doi: 10.3389/FNINS.2016.00005/BIBTEX. [PubMed: 26858587]

[52]. Baek H and Kim H, "Anesthetic depth challenges for ultrasonic neuromodulation: An electroencephalographic index monitoring," J Ther Ultrasound, 2016.

[53]. Hellman A et al. , "Pilot study on the effects of low intensity focused ultrasound in a swine model of neuropathic pain," J Neurosurg, vol. 135, no. 5, pp. 1508–1515, Apr. 2021, doi: 10.3171/2020.9.JNS202962.

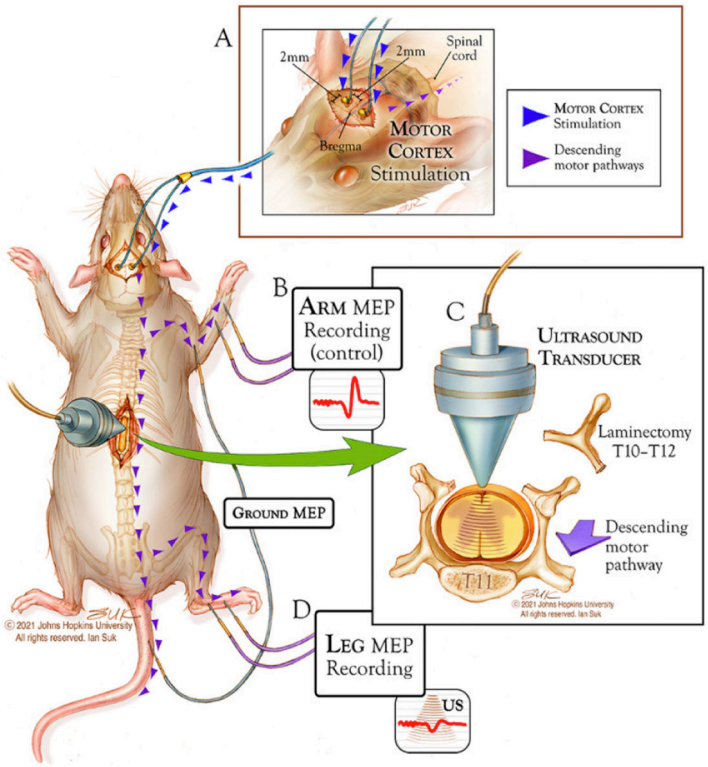

Figure 1.

Illustration of the animal model. **(A)** Cranial electrodes placed 2 mm posterior and lateral from the bregma. **(B)** Upper extremity electrodes placed in brachioradialis muscle. **(C)** Low-intensity ultrasound placed in direct contact with the dorsum of the spinal cord. **(D)** Lower extremity electrode placed in the soleus muscle.

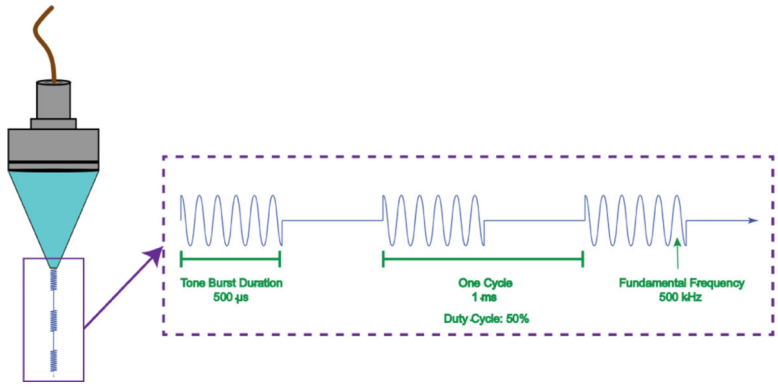

Figure 2.
Depiction of the low-intensity pulsed ultrasound parameters.

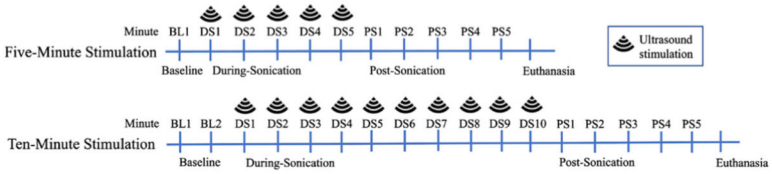

Figure 3.

Experimental set-up. Each experiment trial was separated into multiple 1-minute-windows and each window was named according to the period and its time order.

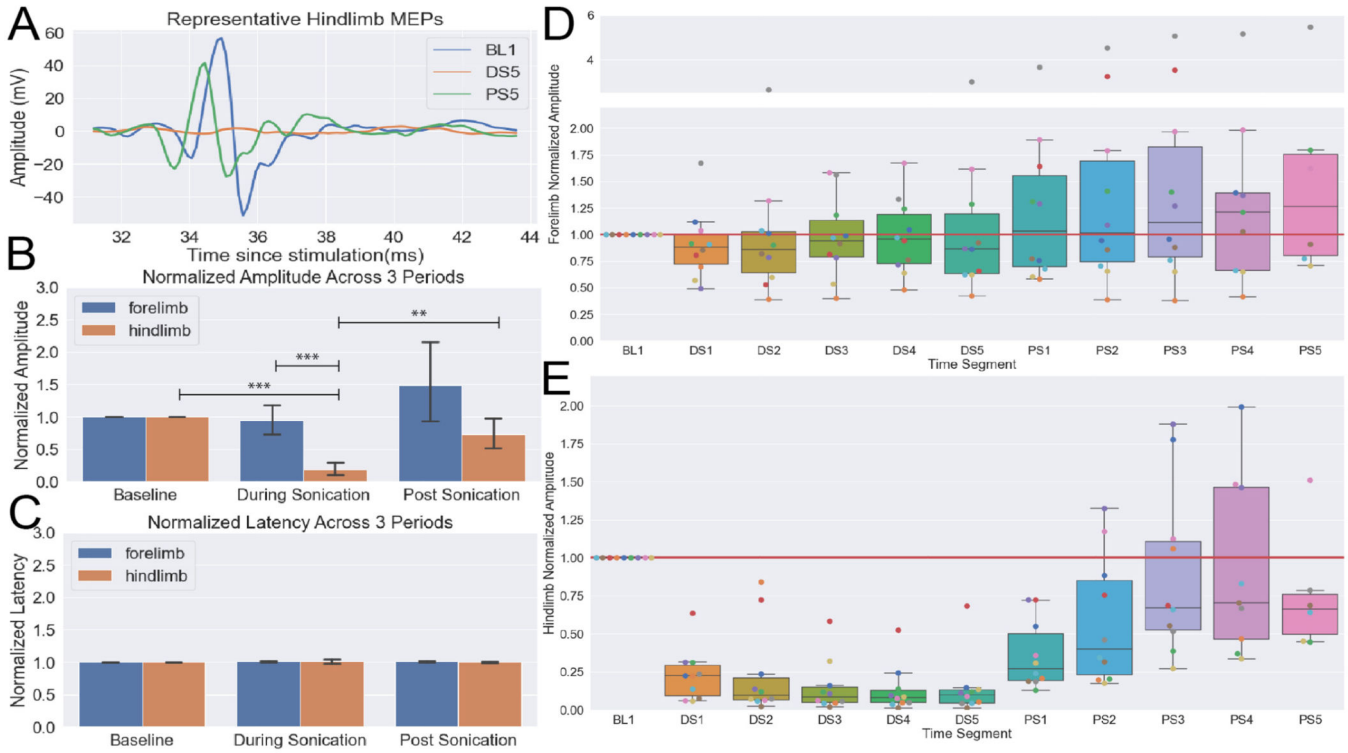

Figure 4.

Results of the 5-min sonication trial. (**A**) Representative motor evoked potential; (**B**) Normalized amplitude across before, during, and post sonication periods; (**C**) Normalized latency across the 3 stages; (**D**) Boxplot of normalized forelimb amplitude; (**E**) Boxplot of normalized hindlimb amplitude. The amplitude was measured from the average MEPs for each 1-min time segment. **, $p < 0.01$, ***, $p < 0.001$. BL: Baseline, DS; During Sonication, PS: Post Sonication. Time segment number corresponds to the minute of sonication or post sonication.

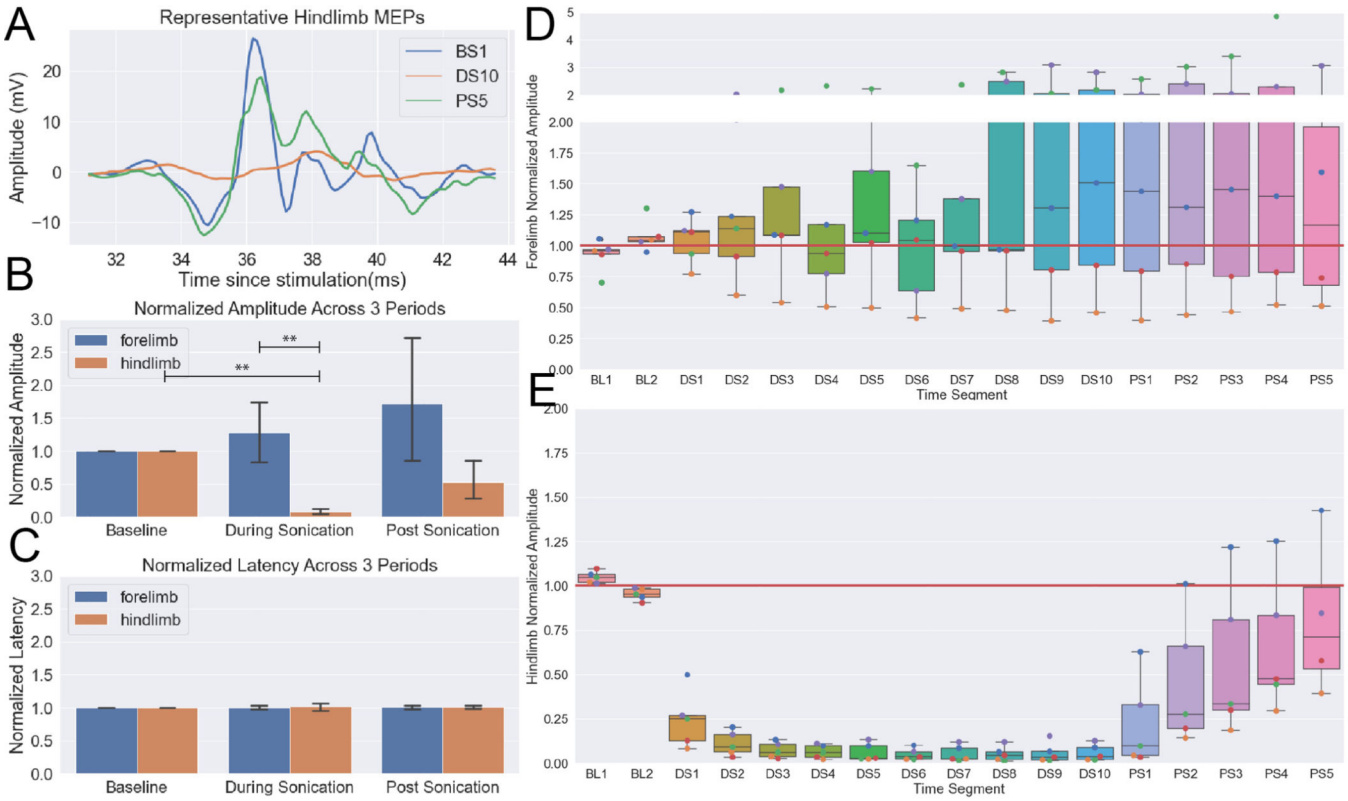

Figure 5.

Results for the 10-min sonication trial. (**A**) Representative motor evoked potential; (**B**) Normalized amplitudes before (baseline), during and post sonication; (**C**) Normalized latency for the 3 periods; (**D**) Boxplot of normalized forelimb amplitude; (**E**) Boxplot of normalized hindlimb amplitude. The amplitude was measured from the average MEPs for each 1-min time segment. **, $p < 0.01$, ***, $p < 0.001$. BL: Baseline, DS; During Sonication, PS: Post Sonication. Time segment number corresponds to the minute of sonication or post sonication.

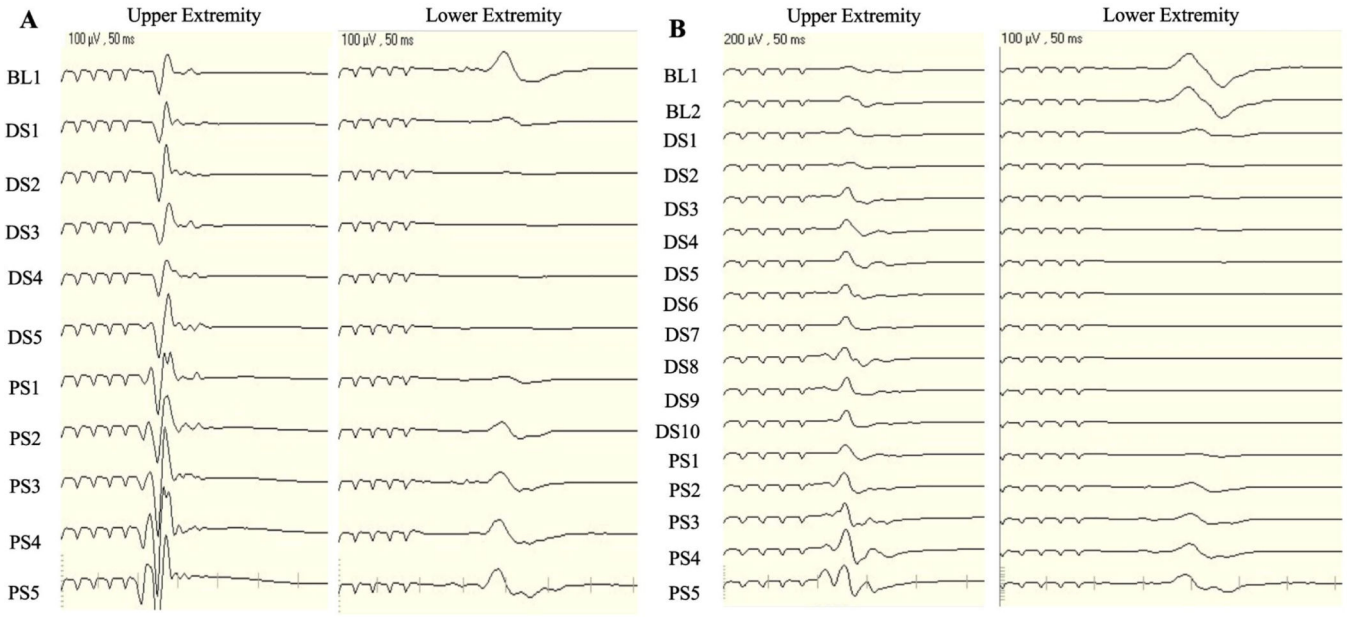

Figure 6.

Depiction of the average MEP waveform during each minute of the trial. (**A**) Waveforms from the 5-min trial. (B) Waveforms from the 10-min trial. BL: Baseline, DS; During Sonication, PS: Post Sonication.

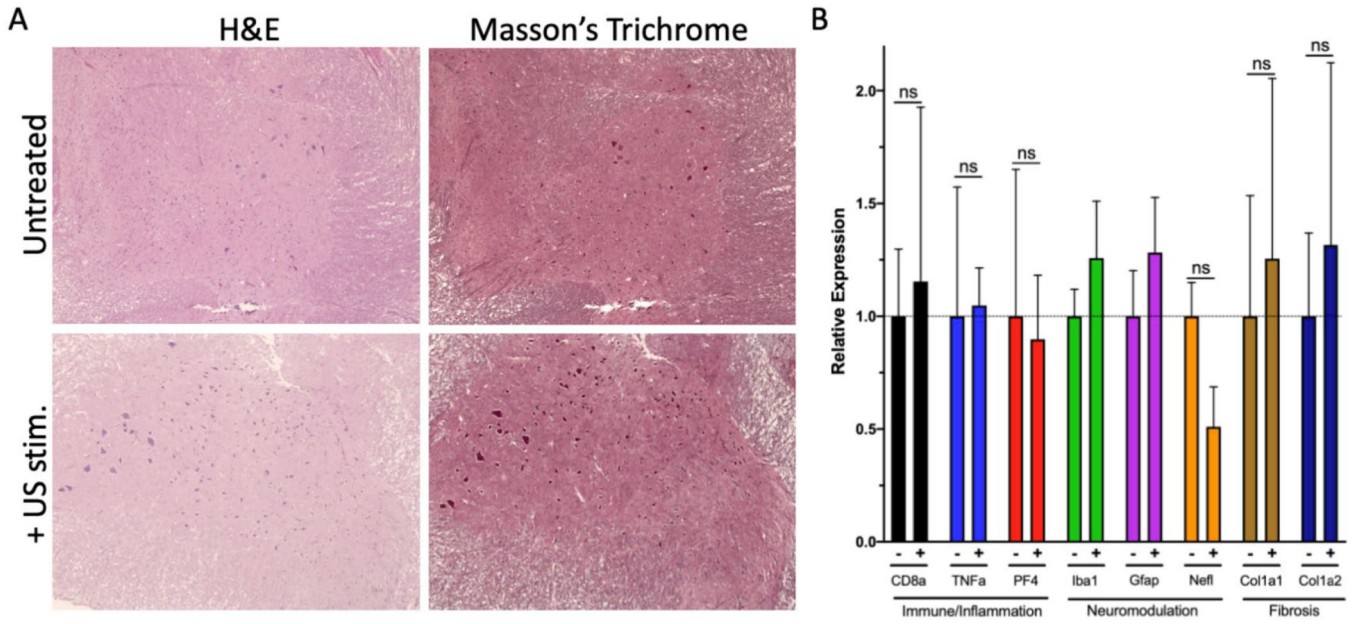

Figure 7.

LIUS does not produce damage to spinal cord as demonstrated with tissue staining and qPCR data. (**A**) Spinal cord samples were collected and stained with H&E and Masson's trichome. These stains show that sonication did not lead to gross tissue deficits, such as hemorrhaging or necrosis. (**B**) qPCR data demonstrates that there is no significant difference in immune/inflammation and fibrosis genes between the control and stimulated groups. ns, not significant. *, $p < 0.05$ (vs. non-stim (−)).

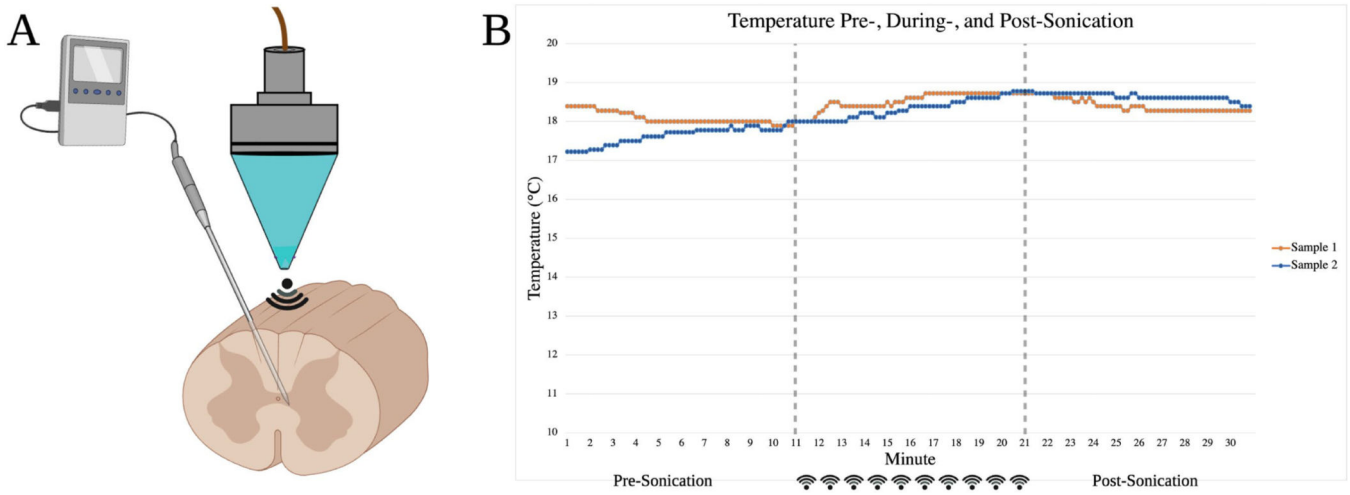

Figure 8.

Temperature change during ten minutes of sonication in two rat *ex vivo* spinal cord samples. (**A**) Depiction of experimental set-up; (**B**) Temperature during pre-, during-, and post-sonication. *Created with* BioRender.com.